THE JOURNAL OF BIOLOGICAL CHEMISTRY VOL. 280, NO. 52, pp. 43224–43235, December 30, 2005

Lack of ABCA1 Considerably Decreases Brain ApoE Level and Increases Amyloid Deposition in APP23 Mice*

Received for publication, April 25, 2005, and in revised form, September 19, 2005 Published, JBC Papers in Press, October 5, 2005, DOI 10.1074/jbc.M504513200

Radosveta Koldamova[‡1,2], **Matthias Staufenbiel**[§], **and Iliya Lefterov**[¶1]

From the [‡]*Department of Pharmacology, University of Pittsburgh School of Medicine, Pittsburgh, Pennsylvania 15261,* [§]*Novartis Institutes of BioMedical Research, CH-4002 Basel, Switzerland, and* [¶]*Department of Environmental and Occupational Health, Graduate School of Public Health, University of Pittsburgh, Pittsburgh, Pennsylvania 15260*

ABCA1 (ATP-binding cassette transporter A1) is a major regulator of cholesterol efflux and high density lipoprotein (HDL) metabolism. Mutations in human *ABCA1* cause severe HDL deficiencies characterized by the virtual absence of apoA-I and HDL and prevalent atherosclerosis. Recently, it has been reported that the lack of ABCA1 causes a significant reduction of apoE protein level in the brain of ABCA1 knock-out (ABCA1$^{-/-}$) mice. ApoE isoforms strongly affect Alzheimer disease (AD) pathology and risk. To determine further the effect of ABCA1 on amyloid deposition, we used APP23 transgenic mice in which the human familial Swedish AD mutant is expressed only in neurons. We demonstrated that the targeted disruption of *ABCA1* increases amyloid deposition in APP23 mice, and the effect is manifested by an increased level of Aβ immunoreactivity, as well as thioflavine S-positive plaques in brain parenchyma. We found that the lack of ABCA1 also considerably increased the level of cerebral amyloid angiopathy and exacerbated cerebral amyloid angiopathy-related microhemorrhage in APP23/ABCA1$^{-/-}$ mice. Remarkably, the elevation in parenchymal and vascular amyloid in APP23/ABCA1$^{-/-}$ mice was accompanied by a dramatic decrease in the level of soluble brain apoE, although insoluble apoE was not changed. The elevation of insoluble Aβ fraction in old APP23/ABCA1$^{-/-}$ mice, accompanied by a lack of changes in APP processing and soluble β-amyloid in young APP23/ABCA1$^{-/-}$ animals, supports the conclusion that the ABCA1 deficiency increases amyloid deposition. These results suggest that ABCA1 plays a role in the pathogenesis of parenchymal and cerebrovascular amyloid pathology and thus may be considered a therapeutic target in AD.

The deposition of Aβ[3] in the brain parenchyma and vessels is a pathological hallmark of AD, and it is believed that Aβ plays a central role in the pathogenesis of the neuronal dysfunction and cognitive impairment during the progression of the disease. Unlike familial early onset forms of AD, which are caused by mutations in APP or presenilins, the cause of late onset AD (LOAD) remains unknown. The inheritance of the *apoE* ϵ4 allele (apoE4) is considered a strong and independent risk factor of AD and is associated with increased neuritic plaques and CAA (1–3). It has been reported that in APP transgenic mice the disruption of the *apoE* gene causes a dramatic reduction of parenchymal amyloid plaques and CAA (4–6).

Two independent groups have reported recently that the lack of ABCA1 causes >75% reduction of apoE protein level in the brain of ABCA1$^{-/-}$ mice (7, 8). The decreased apoE level in the central nervous system was not related to *apoE* gene expression but likely was caused by increased metabolism of abnormally lipidated apoE containing lipoprotein (8). ABCA1 is a major regulator of cholesterol efflux, HDL metabolism, and reverse cholesterol transport (9, 10). Mutations in the *ABCA1* gene cause severe HDL deficiencies, the most prominent of which is Tangier disease, which is characterized by the virtual absence of apoA-I and HDL, the accumulation of cholesterol in cells, and the prevalence of atherosclerosis (11–13). The transcriptional activation of ABCA1, and other genes involved in cholesterol metabolism, is controlled by nuclear liver X receptors α and β LXRα/β (14, 15). Target genes of LXRα/β have already been implicated in the control of APP proteolytic processing (16–18). The effect was attributed primarily but not only to ABCA1. It was also reported that a set of genetic variants of ABCA1 modifies the risk for AD (19, 20) in Scottish, Swedish, and English populations, although another study of American and UK populations found that ABCA1 variants do not appear to influence the risk of LOAD (21). Experiments with any of those genetic variants or complex AD model systems (APP transgenic/ABCA1 knock-out animals for example) have not been reported, and so there is no definitive conclusion about the role of ABCA1 in AD. To determine further the effect of ABCA1 on amyloid deposition, we used APP23 transgenic mice in which APPsw is expressed only in the brain. These mice develop compact amyloid plaques in brain parenchyma and CAA, reminiscent of the pathological features of AD (22–24). In this study APP23 mice were bred to ABCA1 knock-out mice, and Aβ-related pathology was evaluated in APP23 mice with intact (APP23/ABCA1$^{+/+}$) or disrupted (APP23/ABCA1$^{-/-}$) *ABCA1* gene. Our results demonstrate that in APP23 mice the lack of ABCA1 increases Aβ deposition.

MATERIALS AND METHODS

Transgenic Mice—This study fully conformed to the guidelines outlined in the Guide for the Care and Use of Laboratory Animals from the United States Department of Health and Human Services and was approved by the University of Pittsburgh Institutional Animal Care and Use Committee. We used APP23 transgenic mice expressing human familial AD mutant APP751 with Swedish double mutation at positions 670/671 (APPK670N, M671L) (23). The expression of human APPsw is driven by the murine *Thy-1* promoter and is restricted to neurons.

* This work was supported in part by Neurosciences Education and Research Foundation (to R. K.) and NIA Grants AG023662 (to R. K.) and AG023304 (to I. L.) from the National Institutes of Health. The costs of publication of this article were defrayed in part by the payment of page charges. This article must therefore be hereby marked "*advertisement*" in accordance with 18 U.S.C. Section 1734 solely to indicate this fact.

[1] To whom correspondence should be addressed. Dept. of Environmental and Occupational Health, Graduate School of Public Health, University of Pittsburgh, Pittsburgh, PA 15260. Tel.: 412-383-6906; E-mail: radak@pitt.edu or iliyal@pitt.edu.

[2] Present address: Department of Environmental and Occupational Health, University of Pittsburgh, 100 Technology Drive, Pittsburgh, PA 15260.

[3] The abbreviations used are: Aβ, β-amyloid; AD, Alzheimer disease; APP, amyloid precursor protein; APPfl, APPfull-length; sAPP, soluble APP; h, human; CAA, cerebral amyloid angiopathy; CTF, APP carboxyl-terminal fragments; HDL, high density lipoproteins; Thio-S, thioflavine S; WB, Western blotting; ELISA, enzyme-linked immunosorbent assay; PBS, phosphate-buffered saline; CHAPS, 3-[(3-cholamidopropyl)dimethylammonio]-1-propanesulfonic acid; LOAD, late onset AD; LXR, liver X receptor; LRP, low density lipoprotein receptor-related protein.

APP23 (C57BL/6 background) were cross-bred to ABCA1$^{+/-}$ heterozygous mice (DBA/1-Abca1^{tm1Jdm}/J; The Jackson Laboratory) to generate APP23/ABCA1$^{+/-}$ progeny (C57BL/6 × DBA/1). The progeny was identified by PCR, and APP23/ABCA1$^{+/-}$ mice were bred to ABCA1$^{+/-}$ littermates (F1, no APP transgene, mixed C57BL/6 × DBA/1 background) to yield APP23/ABCA1$^{-/-}$, APP23/ABCA1$^{+/-}$, and APP23/ABCA1$^{+/+}$ bigenic littermate mice. All mice used in this study are hemizygous APP23. At weaning, a distortion in the Mendelian inheritance of the APP23/ABCA1$^{-/-}$ genotype was observed that was three times less than expected, suggesting a perinatal lethality of APP23/ABCA1$^{-/-}$ pups. APP23/ABCA1$^{-/-}$ mice appeared normal and weighed slightly less (statistically insignificant) compared with APP23/ABCA1$^{+/+}$ littermates. APP23/ABCA1$^{-/-}$ developed similarly to APP23/ABCA1$^{+/+}$, and no gross anatomical abnormalities were observed until 13 months of age.

Animal Tissue Processing—Mice were anesthetized with pentobarbital (150 mg/kg, intraperitoneal) and perfused transcardially with 100 ml of PBS (0.1 M, pH 7.4). Brains were rapidly removed; the olfactory bulb and cerebellum were deleted and divided in hemibrains. One hemibrain was snap-frozen on dry ice and the other was drop-fixed in 4% phosphate-buffered paraformaldehyde at 4 °C for 48 h.

Antibodies—Rabbit polyclonal anti-ABCA1 antibody was purchased from Novus Biologicals (Littleton, CO). The 6E10 monoclonal antibody (Signet, Dedham, MA) recognizes the first 17 amino acids of the Aβ peptide. 6E10 antibody was used for Western blotting (WB) to detect full-length human APP and sAPPα. Rabbit C8 polyclonal antibody (25) was used to detect CTF resulting from α- or β-secretase cleavages. Rabbit 869 antibody (25) was used to detect sAPPβ by WB. This antibody does not recognize full-length APP but recognizes the neoepitope generated after cleavage by β-secretase. Murine-specific apoE antibody was from Santa Cruz Biotechnology (Santa Cruz, CA). TAU-5 antibody (NeoMarkers, Fremont, CA) is a phospho-independent antibody that recognizes total tau protein. Glyceraldehyde-3-phosphate dehydrogenase monoclonal antibody was purchased from Chemicon International (Temecula, CA). Secondary antibodies conjugated to horseradish peroxidase were from Jackson ImmunoResearch (West Grove, PA).

Histology and Immunohistochemistry—HistoPrep (Fisher)-embedded hemibrains were cut in the coronal plane at 30 μm on a cryostat. Sections were selected 300 μm apart, starting from a randomly chosen section about 300 μm caudal from the first appearance of CA3 and the dentate gyrus. The immunostaining procedure was performed on floating sections as described by Matsuoka *et al.* (26). Briefly, after washing in PBS containing 0.2% Triton X-100 (PBST), nonspecific binding was blocked by incubating the sections in PBST, 3% normal goat serum (Vector Laboratories) for 1 h before the incubation in biotinylated 6E10 at 4 °C overnight. Sections were then washed in PBST and incubated in ABC Elite reagent (Vector Laboratories), and immunoreactivity was visualized by using diaminobenzidene/nickel (DAB/Ni). The specificity of immunoreactivity was confirmed by the lack of signal when applying the same protocol on brain sections from nontransgenic wild type littermates. For thioflavine S (Thio-S) staining, floating sections were washed in PBST, mounted on Superfrost Plus slides (Fisher), coated with Vectabond (Vector Laboratories), and processed essentially as described previously (27). Sections mounted on the slides were postfixed in 10% formalin for 10 min, washed in PBS, incubated in 0.25% potassium permanganate for 10 min, treated with 2% potassium metabisulfite, 1% oxalic acid until they appeared white, and finally stained for 10 min in 0.015% Thio-S in 50% ethanol. After washing in 50% ethanol and water, the slides were dried and dipped into Histo-Clear before being coverslipped with Permount. All chemicals were from Sigma at the highest recommended grade of purity.

Parenchymal and cerebrovascular amyloidoses were evaluated on the same sections but were recorded and presented separately. Microscopic examinations were carried out using Leica DM fluorescent microscope and images captured by CCD camera (DG 300F, Leica). For quantitative analysis, Aβ and amyloid deposition in the neocortex and hippocampus was defined as the percent area covered by Aβ immunoreactivity (% Aβ load) and Thio-S positivity (% Thio-S load), respectively. For each mouse, Aβ immunoreactivity or Thio-S-positive plaques were counted in 6–7 sections per hemibrain 300 μm apart at a magnification of 50. The percentage of area covered by Aβ-IR or Thio-S positivity was determined by examining the entire area of the section using IPLab 3.1 software.

Cerebrovascular amyloidosis was evaluated on Thio-S-stained slides in pia, cortex, hippocampus, and thalamus, using the same approach and presented as % vascular amyloid.

A qualitative rating scale of CAA severity, similar to that reported previously for APP23 mice was used (28) as follows: severity grade 1, with amyloid confined to the vessel wall; severity grade 2, vascular amyloid with amyloid infiltrating the surrounding neuropil; and severity grade 3, dyshoric amyloid with amyloid deposition within the vessel wall and with a thick and complete amyloid coat around the vessel wall. A set of seven coronal sections/mouse equally spaced throughout the brain was evaluated, and Thio-S-positive vessel surface area was measured in each of four regions (pia, cortex, hippocampus, and thalamus). It should, however, be stated that because coronal sections were used in all cases, this value may be influenced by vessel orientation (*e.g.* if vessels that run perpendicular to the plane of section were more likely to contain fibrillar amyloid, the reported percentage would be an underestimate of the total affected surface area).

Quantitation of Cerebral Hemorrhage—30-μm sections were mounted on microscopic slides, fixed for 10 min in 10% freshly prepared formalin, and processed according to Carson (29). The slides were well rinsed in distilled water, incubated in Perl's solution, equal parts of 2% potassium ferrocyanide and 2% hydrochloric acid, and rinsed again. The sections were counterstained with Nuclear Fast Red (Vector Laboratories) for 5 min, rinsed under running tap water for 5 min, and coverslipped. All sections were scanned using 5× objective and focal hemorrhages analyzed and counted at ×250. The numbers of Perl's Berlin blue-stained clusters of hemosiderin staining (or Prussian blue-positive sites) were counted on all sections, and the average number of sites per section was quantified. A set of six equally spaced sections throughout the neocortex, hippocampus, and thalamus were examined, and the number of positive profiles was determined and averaged to a per section value.

Tissue Homogenizing and Western Blotting—The frozen hemibrains (only cortices and hippocampi) were homogenized in tissue homogenization buffer (THB) (250 mM sucrose, 20 mM Tris base, 1 mM EDTA, 1 mM EGTA, 1 ml per 150 mg of tissue) and protease inhibitors essentially as described before (25). Protein extracts were prepared by 1:1 dilution of the initial homogenate with 2× RIPA buffer (10 mM Tris-HCl, pH 7.3, 1 mM $MgCl_2$, and 0.25% SDS, 1% Triton X-100) in the presence of protease inhibitors (10 μg/ml leupeptin, 10 μg/ml aprotinin, and 10 μg/ml 4-(2-aminoethyl)benzenesulfonyl fluoride) and sonication. WB for ABCA1, APPfl, and CTFα/β were made as described previously (25). sAPPα and sAPPβ were determined by WB in soluble extracts prepared from brain homogenate using cold 0.4% diethylamine in 100 mM NaCl, centrifuged at 135,000 × *g* for 1 h at 4 °C, and neutralized by adding 0.5 M Tris-HCl, pH 6.8.

Aβ ELISA—Soluble Aβ was extracted with 2× RIPA buffer and centrifuged at 135,000 × *g*. Insoluble Aβ was extracted from the resulting pellet using 70% ice-cold formic acid. The soluble and insoluble Aβ extracts were additionally diluted in EC buffer (20 mM sodium phosphate, 2 mM EDTA, 400 mM NaCl, 0.2% bovine serum albumin, 0.05% CHAPS, 0.4% Block Ace, 0.05% NaN_3, pH 7.0), and $Aβ_{1-40}$ and $Aβ_{1-42}$ concentrations were measured by sandwich ELISA as described previously (25). Briefly, ELISA for Aβ was performed using 6E10 as the capture antibody, and anti-Aβ40 (G2-10 monoclonal antibody) and anti-Aβ42 (G2-13 monoclonal antibody) monoclonal antibodies conjugated to horseradish peroxidase (Genetics Co., Schlieren, Switzerland) were used as the detection antibodies. The reaction was developed by TMB Microwell peroxidase substrate system (Kierkegaard & Perry Laboratories, Gaithersburg, MD). The final values of Aβ were based on $Aβ_{1-40}$ and $Aβ_{1-42}$ peptide standards (Bachem Biosciences, King of Prussia, PA). The amount of Aβ was normalized either to the total protein or to the expression of APPfl as measured by WB and was expressed as picomoles/mg.

WB for insoluble Aβ was performed using 10 μl of formic acid-extracted Aβ. The solvent (formic acid) was evaporated, and the pellet was resuspended in 2× NuPAGE loading buffer. The proteins were resolved on 4–12% NuPAGE gels and transferred on the nitrocellulose membranes. Membranes were boiled for 5 min in PBS, and $Aβ_{total}$ was detected with 1:1000 dilution of 6E10 antibody.

WB for Soluble and Insoluble ApoE—The soluble apoE was extracted from brain homogenates using 2× RIPA buffer and sonication and was centrifuged at 135,000 × *g*. The insoluble pellet was dissolved in 70% formic acid, sonicated for 30 s, and centrifuged at 135,000 × *g*. WB for soluble and insoluble apoE were made using 30 μg of total protein. For insoluble apoE, formic acid was evaporated (as for Aβ WB), and the pellet was resuspended in 2× NuPAGE loading buffer. For soluble and insoluble apoE, the proteins were resolved on 4–12% NuPAGE gels and transferred on the nitrocellulose membranes. Insoluble apoE was detected with a 1:100 dilution of anti-mouse apoE antibody, and soluble apoE was detected with 1:500 dilution of the same antibody. To avoid stripping and re-probing of the membranes for a loading control, we used anti-tau antibody Tau5, which is phospho-independent and recognizes total tau (55–65 kDa).

Statistical Analysis—Results are reported as means ± S.E. Statistical significance was determined by two-tailed Student's *t* test or Mann-Whitney test. We used Spearman correlations to determine the unadjusted relationships between continuous variables (GraphPad Prism software, Windows version 3.0, San Diego).

RESULTS

ABCA1 Deficiency Does Not Affect the Expression of Human APP but Substantially Decreases Brain ApoE Level in APP23 Mice—To determine the effect of genetically engineered disruption of ABCA1 on Aβ deposition in APP23 transgenic mice, we generated APP23/ABCA1$^{-/-}$ animals. In this study we examined the following 13-month-old bigenic animals: APP23/ABCA1$^{-/-}$ (9 mice, 5 females and 4 males), APP23/ABCA1$^{+/-}$ (16 mice, 13 females and 3 males), and their wild type APP23/ABCA1$^{+/+}$ littermates (14 mice, 7 females and 7 males). We first evaluated the expression of ABCA1 and full-length human amyloid precursor protein (hAPPfl) by Western blotting in aliquots of SDS extracts of cortices and hippocampi. As expected, the results proved that ABCA1 protein expression in APP23/ABCA1$^{-/+}$ mice is reduced by 50% as compared with APP23/ABCA1$^{+/+}$ and is absent in APP23/ABCA1$^{-/-}$ mice (Fig. 1*A*, *upper panel*). ABCA1 deletion did not influence human APPsw transgene expression (751 amino acids, "Swedish" isoform) (Fig. 1*A*, *lower panel*). Because ABCA1 deficiency as reported considerably decreases the amount of endogenous apoE protein in the brains of ABCA1$^{-/-}$ mice (7, 8), we determined the level of soluble (RIPA-extractable) apoE. In confirmation of the previous studies, we found that the level of soluble apoE in 13-month-old APP23/ABCA1$^{-/-}$ mice was reduced more than 70% when compared with APP23/ABCA1$^{+/+}$ (Fig. 1*B*). The same decrease was observed in 3-month-old APP23/ABCA1$^{-/-}$ mice (data not shown).

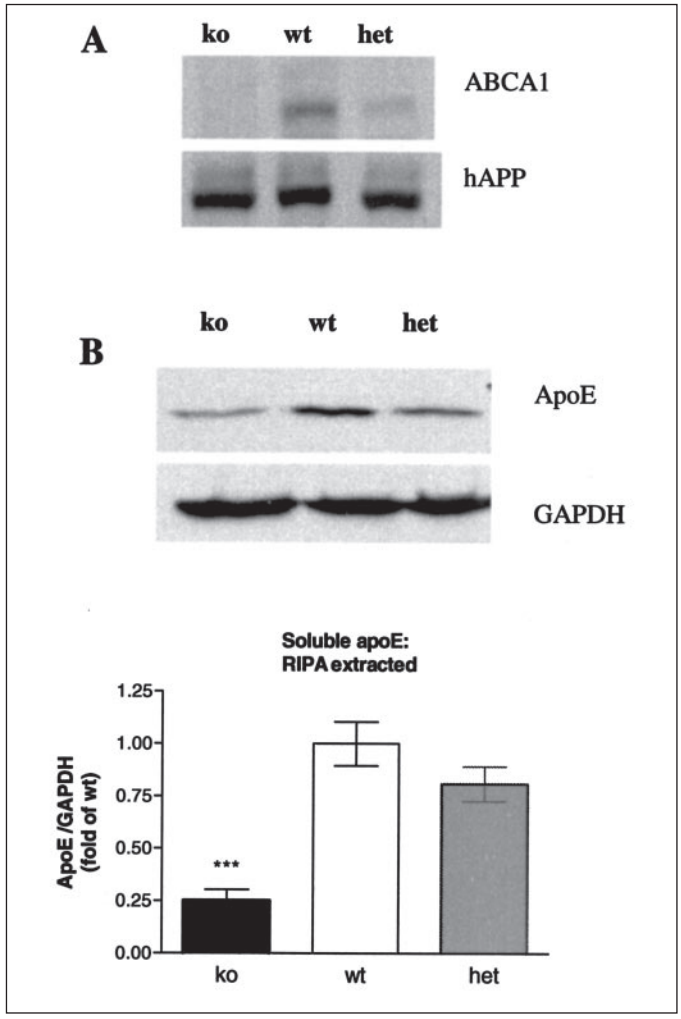

FIGURE 1. **Analysis of ABCA1, APP, and apoE expression in the brain of 13-month-old APP23/ABCA1$^{+/+}$, APP23/ABCA1$^{-/+}$, and APP23/ABCA1$^{-/-}$ mice.** Each lane was loaded with 100 μg (for ABCA1 and APP) or 30 μg (for apoE) of total protein from RIPA-extracted cortices and hippocampi, and the expression of mouse ABCA1, full-length human APPsw (hAPPsw), and mouse apoE was determined by Western blotting. *A*, representative Western blots from APP23/ABCA1$^{+/+}$, APP23/ABCA1$^{-/+}$, and APP23/ABCA1$^{-/-}$ mice demonstrate ABCA1 (*upper panel*) and hAPPsw (*lower panel*) expression. Note the lack of ABCA1 signal in APP23/ABCA1$^{-/-}$ (*ko*) mice. The expression of ABCA1 in APP23/ABCA1$^{-/+}$ mice (*het*) is 2-fold less than in APP23/ABCA1$^{+/+}$ (*wt*) mice. There is no change in the expression of human APPsw (*hAPP*) as detected by 6E10 antibody. *B*, substantial reduction of ApoE levels in the cortex and hippocampus of APP23/ABCA1$^{-/-}$ mice as compared with APP23/ABCA1$^{+/+}$ and APP23/ABCA1$^{-/+}$. ApoE protein was determined by WB using a polyclonal antibody against murine apoE (*upper panel*), and representative WB from APP23/ABCA1$^{+/+}$, APP23/ABCA1$^{-/+}$, and APP23/ABCA1$^{-/-}$ mice are shown. Glyceraldehyde-3-phosphate dehydrogenase (*GAPDH*) (*lower panel*) was used to control for equal protein loading and for normalization. The graph represents means ± S.E. of at least two independent experiments. $n = 14$ for APP23/ABCA1$^{+/+}$, $n = 16$ for APP23/ABCA1$^{-/+}$, and $n = 9$ for APP23/ABCA1$^{-/-}$ mice. Statistics were performed by two-tailed Student's *t* test.

Lack of ABCA1 Increases the Level of Insoluble Aβ in 13-Month-old APP23 Mice—Next we examined whether the deficiency of ABCA1 could alter brain Aβ levels in APP23/ABCA1$^{-/-}$ mice. We measured levels of $Aβ_{40}$ and $Aβ_{42}$ in both RIPA-soluble and -insoluble brain

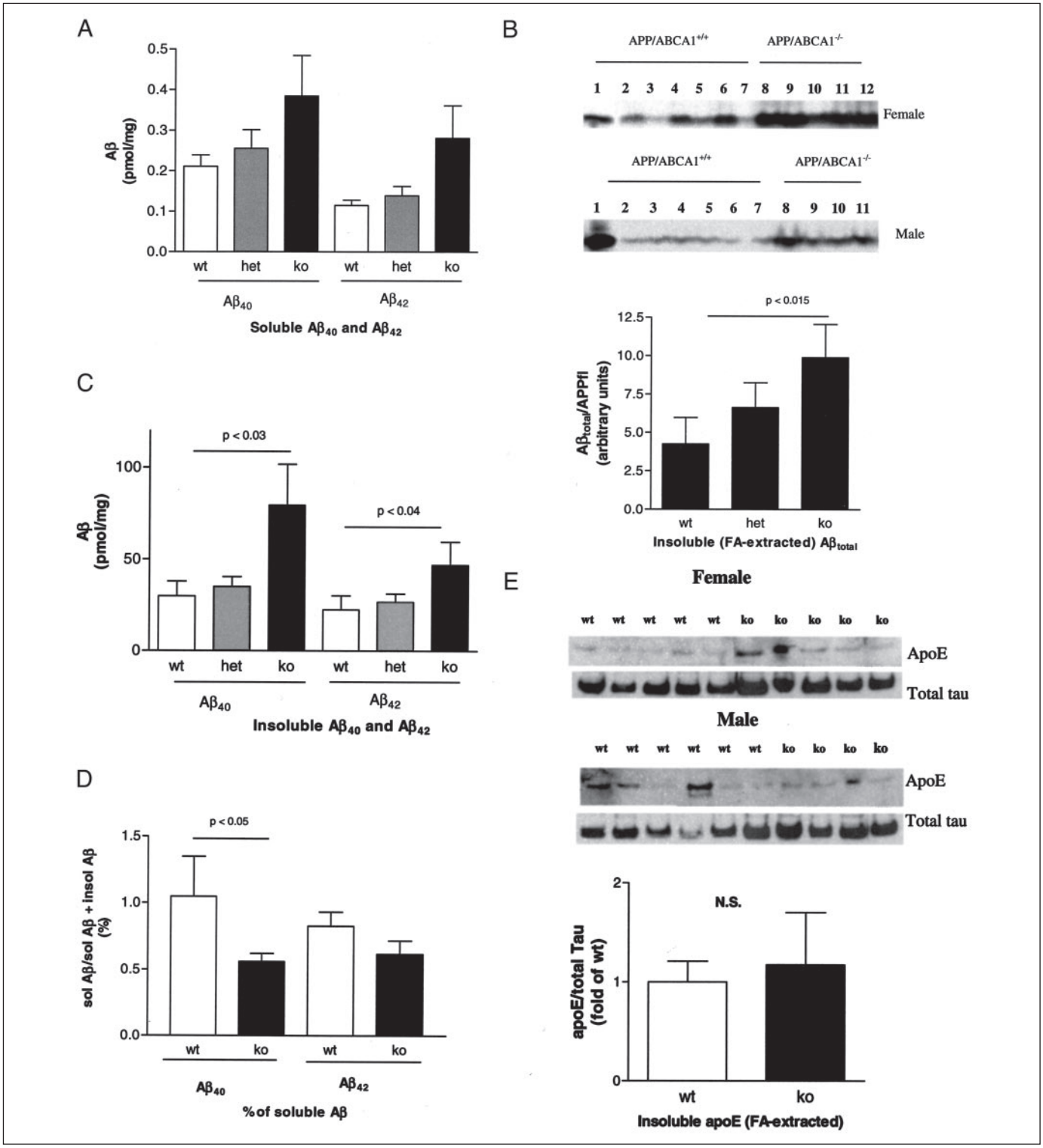

FIGURE 2. **Lack of ABCA1 increases insoluble Aβ_{40} and Aβ_{42} levels in aged APP23/ABCA1$^{-/-}$ mice.** *A–D,* Aβ was extracted first by RIPA (soluble or RIPA-extracted Aβ) followed by formic acid extraction (insoluble or formic acid-extracted Aβ) and was quantified by WB (*B*) or ELISA (*A* and *C*). *A,* soluble Aβ_{40} and Aβ_{42}, as measured by ELISA, were elevated in APP23/ABCA1$^{-/-}$ *versus* APP23/ABCA1$^{+/+}$ and APP23/ABCA1$^{+/-}$ mice; however, the difference did not reach statistical significance. *B,* insoluble Aβ_{total} (Aβ_{40} + Aβ_{42}) was determined by WB of formic acid-extracted Aβ by using 6E10 antibody that recognizes both Aβ_{40} and Aβ_{42} (see text). *Upper panel* is a representative WB of insoluble Aβ_{total} in female mice (*lanes 1–7* are APP23/ABCA1$^{+/+}$ and *lanes 8–12* are APP23/ABCA1$^{-/-}$). *Lower panel* is a representative WB of insoluble Aβ_{total} in male mice (*lanes 1–7* are APP23/ABCA1$^{+/+}$ and *lanes 8–11* are APP23/ABCA1$^{-/-}$). The bands were quantified, and the level of Aβ_{total} was normalized to the level of full-length human APP (*APPfl*). Note the increase of Aβ_{total} in APP23/ABCA1$^{-/-}$ mice *versus* APP23/ABCA1$^{+/+}$ ($p < 0.015$). The graph represents the means ± S.E. of three independent experiments. *C,* insoluble Aβ_{40} and Aβ_{42} as measured by ELISA were increased in APP23/ABCA1$^{-/-}$ *versus* APP23/ABCA1$^{+/+}$ mice. *D,* the percent soluble Aβ_{40} and Aβ_{42} as a fraction of total Aβ (soluble and insoluble) was elevated in APP23/ABCA1$^{+/+}$ *versus* APP23/ABCA1$^{-/-}$ mice. *E,* insoluble apoE was determined by WB of formic acid-extracted brain homogenate (see under "Materials and Methods"). *Upper panel* is a WB of insoluble apoE in female mice, and the *lower panel* is a representative WB of insoluble apoE in male mice. The bands were quantified, and the level of apoE was normalized to the level of total Tau. Values are means ± S.E. of at least two independent experiments. $n = 14$ for APP23/ABCA1$^{+/+}$, $n = 16$ (except for *B*, $n = 14$) for APP23/ABCA1$^{-/+}$, and $n = 9$ for APP23/ABCA1$^{-/-}$ mice. Statistics were performed by Mann-Whitney test. *het,* heterozygous; *wt,* wild type; *ko*, knock-out; *N.S.*, not significant.

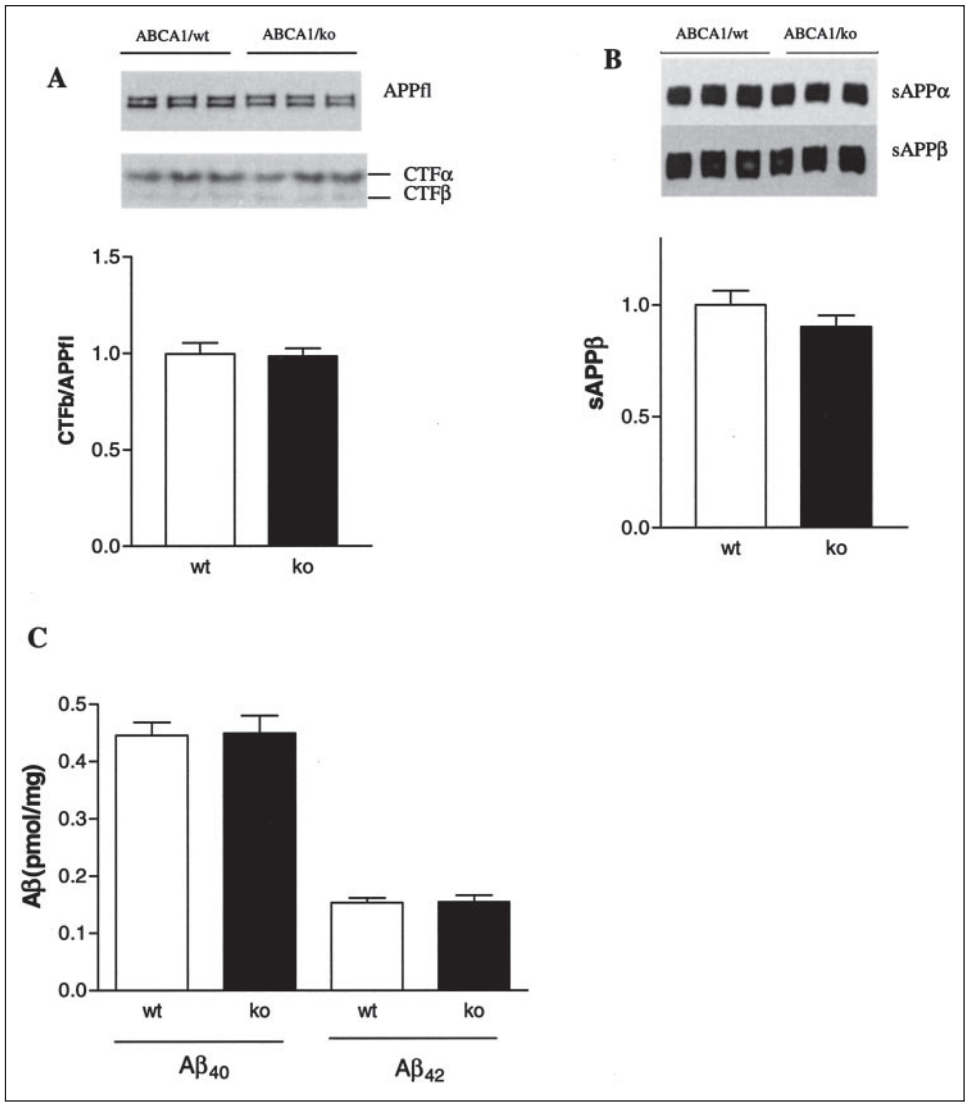

FIGURE 3. **APP processing is not affected in APP23/ABCA1$^{-/-}$.** *A,* CTFα and CTFβ were evaluated in aliquots of RIPA-extracted homogenate and detected with C8 antibody. Representative WB from 13-month-old APP23/ABCA1$^{+/+}$ and APP23/ABCA1$^{-/-}$ mice are shown. The bands were quantified, and the levels of CTFα and CTFβ were normalized to the level of full-length APP (human and endogenous mouse) as determined by the same antibody. The *graph below* represents CTFβ. *B,* sAPPβ and sAPPα were determined by WB in aliquots of diethylamine-extracted cortical and hippocampal homogenates using 869 and 6E10 antibodies, respectively. Representative WB from APP23/ABCA1$^{+/+}$ and APP23/ABCA1$^{-/-}$ mice are shown. The bands were quantified, and the levels of sAPPβ and sAPPα were determined. The *graph below* represents sAPPβ. There was no difference in the levels of sAPPβ and sAPPα, as well as CTFα and CTFβ among the mice of different genotypes. *C,* soluble Aβ_{40} and Aβ_{42} in young 11-week-old mice were measured by ELISA in RIPA-extracted brain homogenate (cortex + hippocampus). There was no difference between APP23/ABCA1$^{-/-}$ and APP23/ABCA1$^{+/+}$ mice. Values are means ± S.E. of at least two independent experiments. *A* and *B* are data from 13-month-old mice. $n = 14$ for APP23/ABCA1$^{+/+}$, $n = 16$ for APP23/ABCA1$^{-/+}$, and $n = 9$ for APP23/ABCA1$^{-/-}$ mice. *C,* data are from 11-week-old mice, $n = 5$ for APP23/ABCA1$^{+/+}$ and APP23/ABCA1$^{-/-}$. Statistics were performed by Mann-Whitney test. *wt,* wild type; *ko,* knock-out.

homogenates of APP23/ABCA1$^{-/-}$ mice, and we compared the values to those in APP23/ABCA1$^{+/+}$ and APP23/ABCA1$^{-/+}$ mice. We found that in APP23/ABCA1$^{-/-}$ *versus* APP23/ABCA1$^{+/+}$ mice, the lack of ABCA1 resulted in an increase of soluble (RIPA-extractable) Aβ_{40} and Aβ_{42}, although the difference did not reach statistical significance (Fig. 2*A*). We also examined the level of insoluble (formic acid extractable) Aβ by WB using 6E10 antibody, which recognizes both Aβ_{40} and Aβ_{42} (referred as Aβ_{total} in Fig. 2*B*). The level of Aβ_{total} showed very high variability among all mice, with male mice (except one animal) having less Aβ_{total} than the female mice. Fig. 2*B* shows that insoluble Aβ_{total} in APP23/ABCA1$^{-/-}$ was increased more than 2-fold ($p < 0.015$ *versus* APP23/ABCA1$^{+/+}$). The level of insoluble Aβ total in APP23/ABCA1$^{-/+}$ mice was intermediate to that in APP23/ABCA1$^{-/-}$ and APP23/ABCA1$^{+/+}$. To assess specifically the proportion of Aβ_{40} and Aβ_{42} in the increased insoluble Aβ, we evaluated their levels by ELISA. The results demonstrated a less than 2-fold increase of insoluble Aβ_{42} in APP23/ABCA1$^{-/-}$ mice ($p < 0.035$ *versus* APP23/ABCA1$^{+/+}$) and a more than 2-fold increase of insoluble Aβ_{40} ($p < 0.025$ *versus* APP23/ABCA1$^{+/+}$, Fig. 2*C*). We concluded that the disruption of ABCA1 in APP23 mice significantly increases the level of insoluble Aβ_{40} and Aβ_{42}. To determine which of the two Aβ forms (soluble or insoluble) is predominantly increased in APP23/ABCA1$^{-/-}$, we measured the percentage of soluble Aβ in the total Aβ (soluble plus insoluble). Fig. 2*D* demonstrates that when compared with APP23/ABCA1$^{+/+}$ mice, the proportion of soluble Aβ_{40} in APP23/ABCA1$^{-/-}$ mice was considerably decreased, suggesting that more Aβ converts from the soluble to the insoluble state in the absence of ABCA1. The difference in the proportion of soluble Aβ_{42} in APP23/ABCA1$^{-/-}$ showed a trend toward a decrease; however, the difference was statistically insignificant. Because it was reported previously that apolipoprotein E co-localized with amyloid plaques in APP transgenic mice (30) and AD brain, we examined apoE level in RIPA-insoluble brain fractions. Insoluble apoE was determined in formic acid-extracted brain fractions, the same used to determine insoluble Aβ. We found a very small amount of apoE in the insoluble fraction (Fig. 2*E*), which was detected only after a longer exposure to x-rays films. There was no difference in the level of insoluble apoE between APP23/ABCA1$^{-/-}$ and APP23/ABCA1$^{+/+}$ mice. The level of insoluble apoE in knock-out mice was 1.1-fold of insoluble apoE in wild type animals, whereas the level of soluble apoE in knock-out mice was 0.25-fold of soluble apoE in wild type mice.

APP Processing Is Not Affected in APP23/ABCA1$^{-/-}$—There can be several reasons for the increased levels of insoluble Aβ in APP23/ABCA1$^{-/-}$ mice, and among them are an increased secretion, impaired clearance, or increased deposition of Aβ. To determine whether the lack

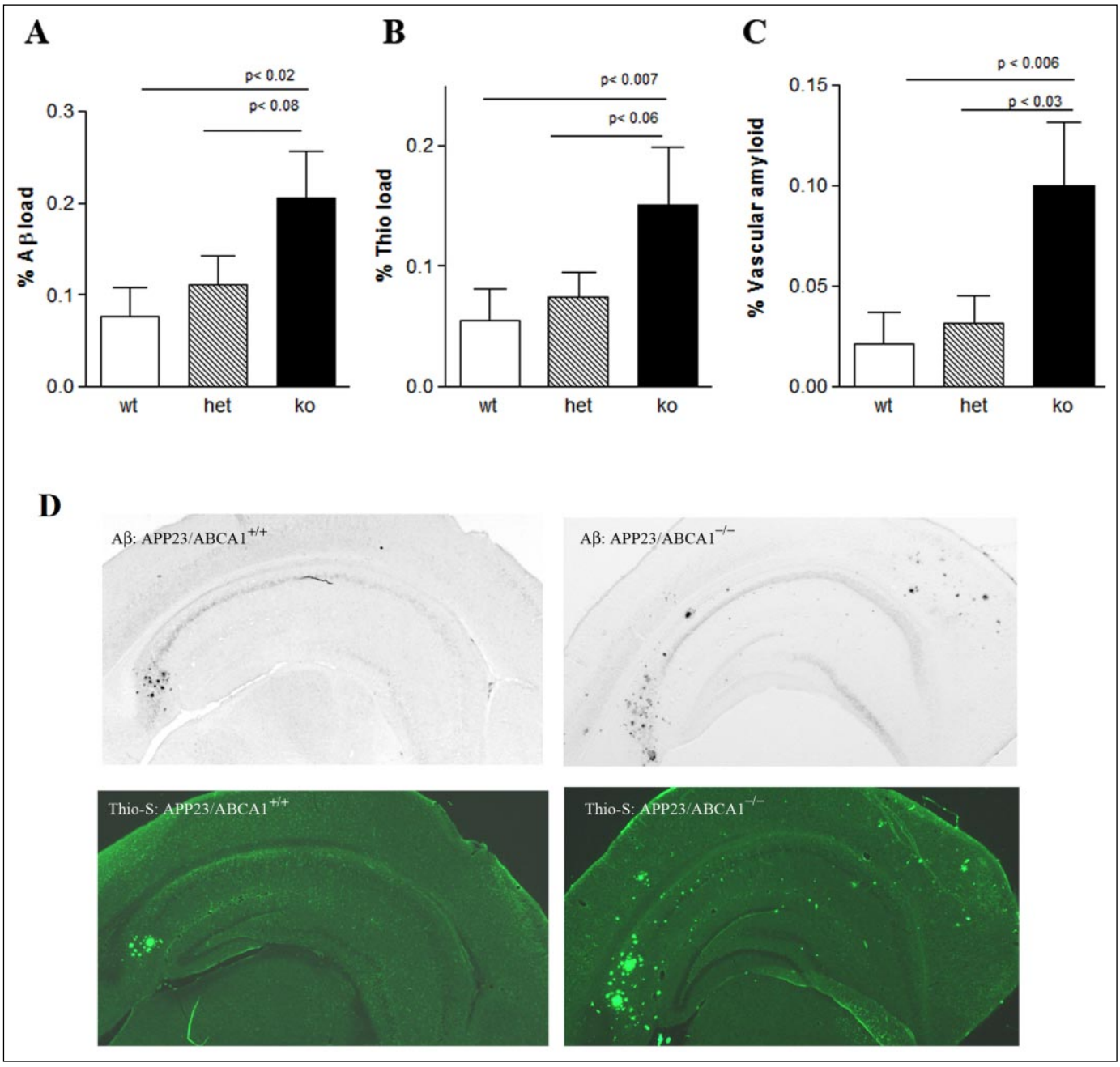

FIGURE 4. **Aβ and Thio-S load in the brain of APP23 mice are increased in the absence of ABCA1.** *A*, percent area of the hippocampus and cortex covered by Aβ immunoreactivity (percent Aβ load) was determined on coronal sections stained with 6E10 antibody. Aβ load is significantly higher in APP23/ABCA1$^{-/-}$ mice as compared with APP23/ABCA1$^{+/+}$ animals. *B*, APP23/ABCA1$^{-/-}$ mice, compared with APP23/ABCA1$^{+/+}$, have significantly greater percent area of the hippocampus and cortex covered by Thio-S-positive staining (percent Thio-S load). *C*, vascular amyloid was determined as percent area occupied by Thio-S-positive leptomeningeal, cortical, hippocampal, and thalamic blood vessels. Note that vascular amyloid in APP23/ABCA1$^{-/-}$ was increased more than 4- and 3-fold as compared with APP23/ABCA1$^{+/+}$ and APP23/ABCA1$^{-/+}$ mice, respectively. *D*, photomicrographs are representative images from APP23/ABCA1$^{+/+}$ and APP23/ABCA1$^{-/-}$ experimental groups of mice. Sections were immunostained with anti-Aβ antibody or stained with Thio-S. Magnification, ×12.5. $n = 13$ for APP23/ABCA1$^{+/+}$, $n = 13$ for APP23/ABCA1$^{-/+}$, and $n = 9$ for APP23/ABCA1$^{-/-}$ mice. *A–C* statistics were performed by Mann-Whitney test. *het*, heterozygous; *wt*, wild type; *ko*, knock-out.

of ABCA1 affects APP processing, we examined the levels of cell-associated carboxyl-terminal fragments (CTFα and CTFβ) as well as the amount of secreted sAPPα and sAPPβ fragments derived after α- or β-secretase cleavages. There was no difference in the quantity of any of those APP fragments in 13-month-old APP23/ABCA1$^{-/-}$ and APP23/ABCA1$^{+/+}$ mice (Fig. 3, *A* and *B*). To determine the level of Aβ before the start of amyloid deposition, we examined $A\beta_{40}$ and $A\beta_{42}$ in young mice (11 weeks old) where all Aβ is in the soluble form (25, 31). The results shown in Fig. 3*C* demonstrate that the lack of ABCA1 did not affect the steady state of Aβ in young mice.

APP23/ABCA1$^{-/-}$ Have Significantly Increased Amyloid Deposition—Next we examined how ABCA1 affects the amyloid deposition in APP23 mice. In the APP23 mice, the first Aβ plaques in brain parenchyma appear at 6 months of age, and all mice develop Aβ deposits at 8 months of age. We found that most of the Aβ plaques are compact (Fig. 4*D*) and can be identified by staining with thioflavine S in agreement with previous reports for these mice (23, 24). Diffuse plaques also occurred, but they were most frequently found in animals with a high plaque burden. Aβ burden (percent area covered by Aβ immunoreactivity) was evaluated by quantitative immunohistochemistry with the 6E10 antibody (26). The amyloid deposits

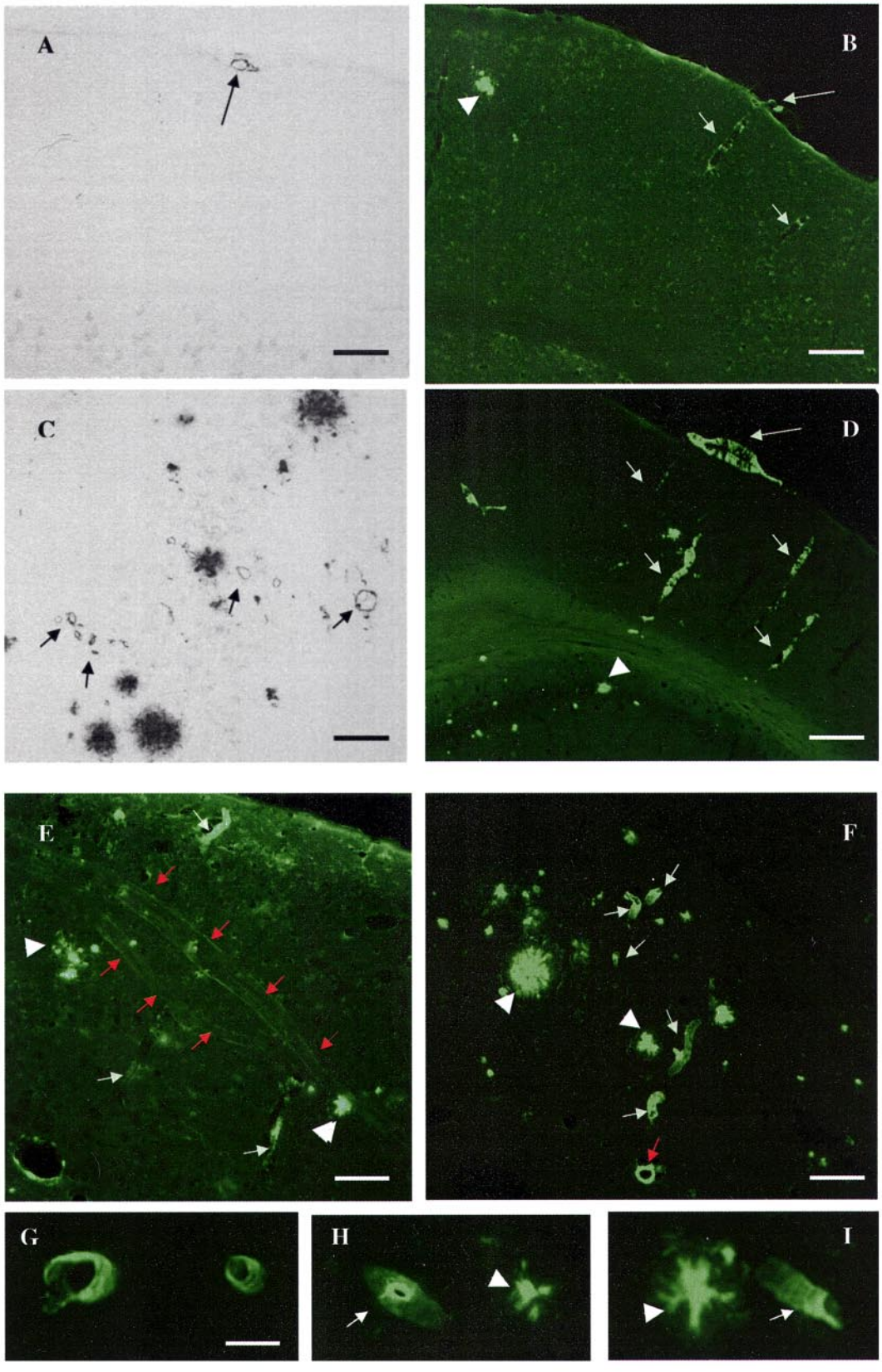

FIGURE 5. **Cerebral amyloid angiopathy is increased in APP23/ABCA1$^{-/-}$ mice.** Aβ (*A*) and Thio-S staining (*B*) in APP23/ABCA1$^{+/+}$ mice reveal engagement predominantly of leptomeningeal (*long arrows*) or neocortical (*short arrows*) blood vessels. All wild type mice had at least few leptomeningeal and some showed penetrating Thio-S-positive cortical vessels. An *arrowhead* in *B* points to a parenchymal plaque. Aβ (*C*) and Thio-S staining (*D–I*) in APP23/ABCA1$^{-/-}$ mice demonstrated vascular amyloid localized in hippocampal (*C, black arrows*), leptomeningeal (*D, long arrows*), neocortical (*D, small arrows*), and thalamic vessels (*G*). Five (out of 9) knock-out mice showed widespread Thio-S-positive vascular amyloid in cortex, similar to that visible in *D,* and four had engagement of hippocampal (as in *C*) and thalamic (as in *G*) vessels. Only one (out of 13) APP23/ABCA1$^{+/+}$ had widespread vascular amyloid in cortex, hippocampus, and thalamus. Within these regions, CAA in APP23/ABCA1$^{-/-}$ mice showed a great variability (*G–I*), ranging from vessels with amyloid confined to the vessel wall (*G*; severity grade 1), to vascular amyloid with amyloid infiltrating the surrounding neuropil (*I*; severity grade 2), and to dyshoric amyloid with amyloid

in APP23/ABCA1$^{+/+}$ were localized predominantly in the neocortex and hippocampus, and plaque loads in neocortex and hippocampus were correlated ($r^2 = 0.67$, $p < 0.001$) as reported previously (32). Lack of ABCA1 did not change the anatomical distribution of Aβ immunoreactivity. Therefore, the presented percentage of Aβ and Thio-S loads encompasses amyloid plaques in the neocortex and hippocampus. Aβ immunoreactivity revealed that the lack of ABCA1 increased the Aβ load more than 2-fold in APP23/ABCA1$^{-/-}$ ($n = 9$) *versus* APP23/ABCA1$^{+/+}$ ($n = 13$; 2.6-fold, $p < 0.019$; Fig. 4, *A* and *D*). There was also a 1.8-fold increase of Aβ burden in APP23/ABCA1$^{-/-}$ compared with the Aβ load in APP23/ABCA1$^{+/-}$ heterozygous mice ($n = 13$), but the difference was statistically insignificant ($p < 0.08$). The quantitation of Aβ load showed a very high variability among APP23 mice with Aβ immunoreactivity occupying from 0.01 to 0.5% of the surface area. To examine closely the effect of ABCA1 on β-amyloid deposition, we divided the mice in groups according to their Aβ load as follows: low with less than 0.1%, medium with more than 0.1%, and high with more than 0.2%. The deficiency of ABCA1 increased the percentage of the mice with high levels of Aβ load as follows: 4 of 9 APP23/ABCA1$^{-/-}$ mice (44%) had an Aβ load more than 0.2%, and only 2 of 13 APP23/ABCA1$^{+/+}$ mice (15%) had a similar β-amyloid load. Accordingly, the percentage of mice with low Aβ load in APP23/ABCA1$^{-/-}$ decreased substantially as follows: 33% of APP23/ABCA1$^{-/-}$ (3 of 9 mice) showed less than 0.1% Aβ load *versus* 76% (10 of 13) among APP23/ABCA1$^{+/+}$ mice.

Earlier it was reported that the absence or even an ~50% reduction of apoE decreases dramatically the Thio-S-positive plaques or fibrillar amyloid (5, 33, 34). Therefore, we were interested to see how the lack of ABCA1 and thus a decreased amount of soluble apoE in the brains of APP23/ABCA1$^{-/-}$ mice would affect a Thio-S-positive load. Most surprisingly, regardless of the considerable decrease in apoE level, the percentage of Thio-S-positive plaques in APP23/ABCA1$^{-/-}$ mice was increased almost 3-fold compared with those in APP23/ABCA1$^{+/+}$ ($p < 0.007$, Fig. 4, *B* and *D*). Moreover, as seen with the Aβ load, the lack of ABCA1 substantially increased the number of the mice with high Thio-S-positive load as follows: in 4 of 9 (44%) APP23/ABCA1$^{-/-}$ mice the Thio S load was more than 0.1%, and only 2 of 13 APP23/ABCA1$^{+/+}$ mice (15%) had the same value of Thio-S load. Accordingly, the number of the mice with low Thio-S load substantially differed in the two groups: whereas 7 of 13 APP23/ABCA1$^{+/+}$ mice (53%) had Thio-S burden less than 0.02%, none of APP23/ABCA1$^{-/-}$ mice had such a low level.

CAA Is Increased in APP23/ABCA1$^{-/-}$ Mice—APP23 develop significant deposition of Aβ in the cerebral vasculature predominantly found in pial, thalamic, cortical, and hippocampal vessels (28, 35). A previous report demonstrated that with aging in 14–22-month-old APP23 mice, there was a pronounced increase in CAA, with detectable Aβ accumulation in vessels occurring slightly later than the first plaques (35). Therefore, we examined how the lack of ABCA1 affects vascular amyloidosis by examining Thio-S load in leptomeningeal, neocortical, and thalamic vessels in 13-month-old APP23/ABCA1$^{-/-}$ and APP23/ABCA1$^{+/+}$ mice. All APP23/ABCA1$^{+/+}$ mice showed vascular amyloidosis detected primarily in leptomeningeal vessels; a few had Thio-S-positive vessels in the cortex, and one mouse (with the highest parenchymal Thio-S load) had numerous vascular amyloid deposits in all examined regions (Fig. 4*C* and Fig. 5, *A* and *B*). In APP23/ABCA1$^{+/+}$ mice, vascular amyloid was approximately one-third (37%) of parenchymal amyloid. As shown in Fig. 4*C*, ABCA1 deficiency increased significantly the level of vascular amyloidosis; APP23/ABCA1$^{-/-}$ mice had more than a 4-fold increase of the area of Thio-S-positive vessels as compared with APP23/ABCA1$^{+/+}$ ($p < 0.006$) and a 3-fold increase over APP23/ABCA1$^{+/-}$ ($p < 0.03$). All APP23/ABCA1$^{-/-}$ mice had vascular deposits in the cortex in addition to leptomeningeal vessels; 5 of 9 mice had a very high level of vascular amyloidosis, and 4 of them showed numerous Thio-S-positive deposits in hippocampal and thalamic vessels. In APP23/ABCA1$^{-/-}$ mice, there was a statistically significant positive correlation between parenchymal and vascular Thio-S load ($r = 0.77$, $p < 0.02$). CAA in APP23/ABCA1$^{-/-}$ mice showed a great variability ranging from vessels with amyloid confined to the vessel wall (Fig. 5*G, severity grade 1*), vascular amyloid with amyloid infiltrating the surrounding neuropil (Fig. 5*I, severity grade 2*), and to dyshoric amyloid with amyloid deposition within the vessel wall and with a thick and complete amyloid coat around the vessel wall (Fig. 5*H*, *arrow, severity grade 3*). The vascular amyloid in APP23/ABCA1$^{-/-}$ was spread predominantly to the medium and small size vessels (Fig. 5, *E*, *F,* and *H*), whereas big vessels were usually not engaged. Fig. 5*E* demonstrates a long vessel through the piriform and lateral part of entorhinal cortices without vascular amyloid deposits. We concluded that lack of ABCA1 increased significantly the CAA in APP23/ABCA1$^{-/-}$ mice.

ABCA1 Deficiency Increases CAA-related Cerebral Hemorrhage in APP23 Mice—The significant increase of cerebrovascular amyloid in APP23/ABCA1$^{-/-}$ mice led us to examine whether the lack of ABCA1 also increased spontaneous hemorrhagic stroke. The conversion of hemoglobin to hemosiderin is the resolution of intracerebral bleeding and requires living cells adjacent to hemorrhage. Blue hemosiderin granules near hemorrhagic lesions appear ~6 days after the lesion, and hemosiderin-positive microglia can be visualized later by Perl's reaction (36). All APP23 mice had focal hemosiderin deposits, most of which were localized to the cytoplasm of perivascular microglial cells. Hemorrhages were localized primarily in the neocortex and pia (and to a lesser degree in the thalamus and hippocampus) and had a distribution very similar to that of CAA. As visible in Fig. 6*C*, the lack of ABCA1 significantly increased the frequency of cerebral hemorrhage in APP23 mice.

DISCUSSION

Senile plaques in AD are extracellular deposits of Aβ peptides, a product of the proteolytic cleavage of APP. Aβ deposition is considered a key pathogenic mechanism in AD, but its cause in sporadic LOAD is still unknown. Epidemiological data suggest that vascular dementia and LOAD share common risk factors, such as hypertension, diabetes, and high plasma cholesterol (37–40). Furthermore, the inheritance of apoE4, a major risk factor for sporadic AD, is associated with increased risk of cerebrovascular disease as well (41).

It is generally accepted that mutations in ABCA1, which is a major regulator of HDL metabolism, increase the risk of atherosclerosis and cardiovascular disease (42). Genetic data support the hypothesis that ABCA1 may have a link to AD through its role in regulating HDL levels. Wollmer *et al.* (20) found that the R219K variant of ABCA1, associated with increased HDL-cholesterol levels and a decreased risk of atherosclerosis (43), delayed the age of onset of LOAD. Regardless that a causal link between atherosclerosis and AD has not been established yet, there

deposition within the vessel wall and with a thick and complete amyloid coat around the vessel wall (*H, arrow*; severity grade 3). The *arrow* in *I* points to a blood vessel, and the *arrowhead* points to a parenchymal plaque. A parenchymal plaque in *H* (*arrowhead*) does not appear to be associated with the vessel (*arrow*). The vascular amyloid in APP23/ABCA1$^{-/-}$ was spread predominantly to the medium and small size vessels (*white arrows* in *E, F,* and *H*), whereas the big vessels were not engaged (*E, red arrows* trace a long vessel through the piriform and lateral part of entorhinal cortices). Note parenchymal amyloid plaques in *E* (*white arrowheads*) arising from or in a close vicinity to the blood vessels. *Scale bars* for *A, C, E,* and *F* are 100 μm, for *B* and *D* are 200 μm, and for *G–I* are 40 μm.

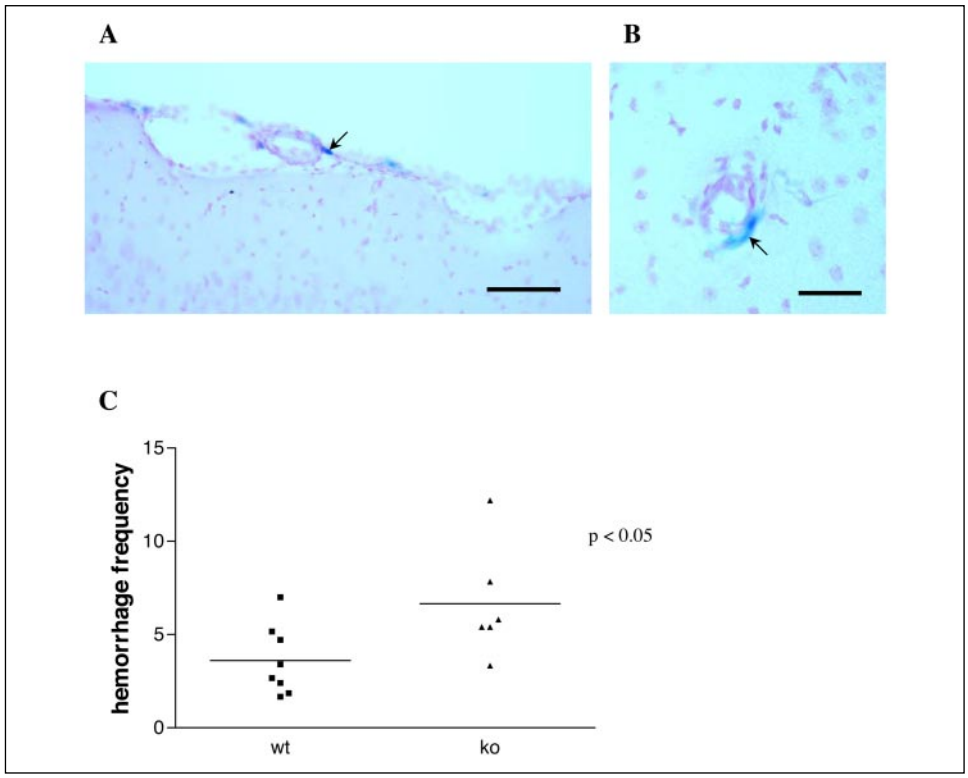

FIGURE 6. **CAA-related hemorrhage is increased in APP23/ABCA1$^{-/-}$ mice.** *A* and *B*, hemosiderin staining (*blue*) in pia (*A*) and the neocortex (*B*) of 13-month-old APP23/ABCA1$^{-/-}$ mouse indicative of old hemorrhage. The sections are counterstained with Nuclear Fast Red. Perivascular hemosiderin-positive microglia (*arrows*) is usually found in close vicinity of blood vessels. Scale bars: for *A* 60 μm, and for *B* 30 μm. *C*, frequency of hemosiderin-positive staining was assessed in six systematically sampled sections through pia, neocortex, hippocampus, and thalamus. Lack of ABCA1 increased CAA-related hemorrhage in *APP23/ABCA1$^{-/-}$* as compared with *APP23/ABCA1$^{+/+}$* mice ($p < 0.03$). $n = 8$ for APP23/ABCA1$^{+/+}$ and $n = 6$ for APP23/ABCA1$^{-/-}$ mice. Statistics were performed by Mann-Whitney test. *wt*, wild type; *ko*, knock-out.

is growing evidence that cerebrovascular dysfunction might be an early event in the mechanisms of AD (44).

In this study we demonstrate that targeted disruption of ABCA1 transporter increases amyloid deposition in APP23 transgenic mice. This effect was manifested by increased levels of Aβ immunoreactivity, as well as Thio-S-positive plaques in brain parenchyma. The lack of ABCA1 also considerably increased the level of vascular amyloid in APP23/ABCA1$^{-/-}$ mice. The elevation of the fraction of insoluble Aβ in old APP23/ABCA1$^{-/-}$ accompanied by no change in soluble Aβ in young APP23/ABCA1$^{-/-}$ mice supports the conclusion that the lack of ABCA1 increases amyloid deposition. Our data are in agreement with two other independent studies demonstrating that ABCA1 deficiency in transgenic mice expressing human APP, harboring different familial AD mutations and under the control of different promoters, increases amyloid deposition. Wahrle and co-workers *et al.* (76) used PDAPP mice (45) and found considerable increase in insoluble Aβ level and trend toward increase of Aβ-immunoreactive deposits. By using the TgSwDI/B transgenic AD model (46), Hirsch-Reinshagen *et al.* (77) demonstrated a substantial increase in Thio-S load in the hippocampus and the thalamus of these mice but no change in total Aβ levels. In the same study, Wellington and co-workers (77) used a second APP transgenic model, APP/PS (47), and found no change in amyloid deposition. All three studies demonstrate a considerable increase in vascular amyloid. The discrepancies in these three reports could be explained by the expression of APP transgenes producing Aβ species with a different ability to aggregate or a different tendency for clearance. It is remarkable, however, that in all three studies the elevation in parenchymal and vascular amyloid was accompanied by a dramatic decrease in soluble apoE levels in the brain. These findings are in contrast with previous experiments in transgenic APP mice with genetically disrupted endogenous mouse apoE (4–6, 33, 34), demonstrating that in APP/apoE$^{-/-}$ mice fibrillar Thio-S-positive Aβ deposits in brain parenchyma and vasculature are virtually missing. Moreover, in transgenic mice expressing human APP driven by two different promoters (PDAPP and Tg-2576 mice), the final effect of apoE disruption was dose-dependent, and apoE$^{-/+}$ animals showed few Thio-S-positive plaques (5, 33, 34).

A possible explanation for the increased Aβ deposition in APP23/ABCA1$^{-/-}$ mice on the background of substantially decreased apoE is that nonfunctional ABCA1 alters APP metabolism, and the result is an increased production of Aβ. Previous *in vitro* data suggested that ABCA1 may affect APP processing. It has been demonstrated, in our studies and in others studies, that LXR ligands up-regulate ABCA1 expression and decrease Aβ secretion (16–18). It should be noted that following LXR ligand treatment in addition to ABCA1 other genes could also have an impact on Aβ secretion. Next, we found an increased level of Aβ_{40} secreted from Tangier fibroblasts that express mutated, nonfunctional ABCA1 protein (25). The data from the present study demonstrate no difference in CTFα and CTFβ and soluble Aβ in young mice if APP23/ABCA1$^{-/-}$ and APP23/ABCA1$^{+/+}$ mice are compared, suggesting that lack of ABCA1 does not affect APP processing. However, at this point we cannot exclude that ABCA1 affects APP processing in a subtle way, and because of a better clearance mechanism in young mice, changes could remain undetected until an older age. Moreover, the results from Wahrle *et al.* (76) show an increase of soluble Aβ at an early age. Previously it was reported that Aβ clearance is an age-dependent process and was significantly decreased in old mice (44, 48). Thus it is possible that the phenotype observed in APP23/ABCA1$^{-/-}$ mice is a consequence of a combination of two defects, which affect APP processing and/or Aβ deposition in two different ways. In our study soluble Aβ in APP23/ABCA1$^{-/-}$ *versus* APP23/ABCA1$^{+/+}$ mice showed a trend toward an increase with age (Fig. 2*A*). Alternatively, the expression of mutated, nonfunctional ABCA1 (as in Tangier disease patients) rather than its complete absence (observed in ABCA1$^{-/-}$ mice) could affect Aβ production and results in a more severe phenotype than complete ABCA1 deficiency. Thus, an expression of nonfunctional ABCA1 in Tangier cells could have a dominant negative effect on

another cellular component that normally limits the secretion of Aβ. Supporting this hypothesis are our previous studies demonstrating that two different familial ABCA1 mutations (T1 and T2 as in Ref. (25)) have a different effect on Aβ secretion in LXR-stimulated and -unstimulated cells (25). Moreover, the clinical phenotypes observed in patients with the above-mentioned ABCA1 mutations were different; patients from the T2 pedigree suffered from premature atherosclerosis, which was not observed in the T1 pedigree. In contrast, one of the two homozygous Tangier patients in the T1 pedigree developed signs of severe dementia and amyloid depositions at age 60 (25).[5] It is obvious that additional *in vitro* studies performed with ABCA1$^{-/-}$ neurons or *in vivo* experiments with transgenic mice expressing mutated human ABCA1 are needed to conclude whether and to what extent ABCA1 has an effect on Aβ secretion.

Alternatively, the lack of ABCA1 in APP23/ABCA1$^{-/-}$ mice and the substantial decrease of apoE and apoA-I could collectively affect Aβ clearance in these animals. ApoE and apoA-I are the two major brain apolipoproteins, with apoE produced by astrocytes and microglia and apoA-I coming from systemic circulation or secreted by brain endothelial cells (49, 50). Binding of Aβ to apolipoproteins (apoE and apoJ) is considered important for its clearance from the brain via low density lipoprotein receptor-related proteins 1 and 2 (LRP1 and LRP2), and it has been shown that Aβ clearance indeed was significantly reduced in young and old apoE knock-out mice (44, 48). A further support for the role of lipoproteins in Aβ clearance is a recent study demonstrating that deletion of apoE and apoJ accelerated Aβ-related pathology in APP transgenic mice (51). It was reported that LRP1 most efficiently removes wild type Aβ_{40}, whereas Aβ_{42} and the Dutch variant of Aβ_{40} containing a higher percentage of β-sheet structures are removed less efficiently (52). Therefore, some of the differences regarding amyloid deposition in the three studies (Wahrle *et al.* (76), Hirsch-Reinshagen *et al.* (77), and this study) could be explained by the differences in the affinity of LRP1 to the prevailing Aβ species in these transgenic models. For example, in PDAPP (76) and APP/PS1 (77), the proportion of Aβ_{42} is higher than in APP23 mice. In Tg-SwDI/B (77), Aβ_{40} is prevailing but contains the Dutch mutation. In addition to Aβ clearance across the blood-brain barrier, the removal of deposited Aβ by astrocytes was demonstrated to depend on apoE, in contrast to astrocytes derived from wild type mice; apoE$^{-/-}$ astrocytes were not able to decrease Aβ load on isolated brain sections (53). However, it should be noted that the binding of apoE to various low density lipoprotein receptors depends on its lipidation status; although lipid-poor apoE could be endocytosed through VLDL (very low density lipoprotein) receptor, delipidated apoE is a poor ligand for LRP and LDL (low density lipoprotein) receptors (54). Previously, it was shown that apoE in the cerebrospinal fluid of ABCA1$^{-/-}$ mice as well as apoE secreted in the conditioned media of ABCA1$^{-/-}$ astrocytes is in a lipid-poor state (7, 8). Therefore, insufficient and poorly lipidated apoE in brain could decrease Aβ clearance and degradation, and its retention in the central nervous system will increase amyloid deposition. Moreover, it was demonstrated that the apoE effect on Aβ aggregation depends on its lipidation status, with lipid-rich apoE being more effective in decreasing Aβ aggregation (55, 56). In confirmation of this hypothesis, we found no change of apoE in the insoluble fraction but a substantial decrease in the soluble fraction. We also demonstrated that the proportion of soluble Aβ as a percentage of total Aβ was decreased in knock-out mice, implying that more Aβ converts from the soluble to insoluble state in the absence of ABCA1. The significant increase of insoluble Aβ in APP23/ABCA1$^{-/-}$ mice is in agreement with the substantial increase of Aβ- and Thio-S-positive deposits.

The role of apoA-I seems less obvious. ApoA-I and HDL bind Aβ *in vitro*, in plasma and cerebrospinal fluid (57, 58). Experiments with neuronal cell lines have shown that apoA-I binding to Aβ decreases its aggregation and toxicity (59, 60). In AD patients decreased plasma apoA-I and HDL concentrations, both observed in ABCA1$^{-/-}$ mice (61), are highly correlated with the severity of Alzheimer disease (62). In addition, as shown by Wahrle *et al.* (8), brain lipoproteins (which normally have characteristics of HDL) had an abnormal structure in the cerebrospinal fluid of ABCA1 knock-out mice. ApoA-I itself may regulate apoE levels in brain interstitium; a recent report showed that apoA-I facilitates apoE recycling in macrophages, thus decreasing its intracellular degradation (63). In mice with disrupted ABCA1, the virtual absence of apoA-I could affect the level of functional apoE and its stability. However, opposing the role of apoA-I in AD is a recent report showing that the lack of apoA-I in APP transgenic mice did not affect amyloid deposition (64). ApoA-I, which is not a ligand for low density lipoprotein receptors and obviously could not participate in Aβ clearance through LRP1, binds other scavenger receptors such as scavenger receptor-B1 and CD36 that have been implicated in the phagocytosis of Aβ (65, 66). Scavenger receptors are localized on the cell surface of astrocytes, microglia, and endothelial cells, and their expression is increased in APP23 mice (67).

Finally, the lack of ABCA1 itself may have a role in increasing amyloid deposition. ABCA1 was implicated in the process of phagocytosis and engulfment of apoptotic bodies probably through the regulation of membrane dynamics (68). A very recent study demonstrates that nematode homologs of ABCA1 (CED-7) and LRP (CED-1) are required for phagocytosis of apoptotic cells in *Caenorhabditis elegans* (69). Therefore, ABCA1, which is expressed in smooth muscle and endothelial cells (70) as well as in astrocytes and microglia (16), may participate in the process of removing Aβ via phagocytosis.

The pathogenesis of CAA and CAA-related hemorrhage in APP mice is not clear. In humans it has been suggested that increased Aβ production by smooth muscle cells leads to smooth muscle degeneration (71). However, this cannot be the case in APP23 (28, 35) or Tg-SwDI/B mice (72) because transgenic Aβ in these mice is of neuronal origin. Previously, it was demonstrated that fibrillar Aβ is toxic for smooth muscle cells (73). Therefore, it is possible that the increase of insoluble Aβ in APP23/ABCA1$^{-/-}$ mice aggravates the degeneration of smooth muscle cells already observed in APP23 mice, thus increasing CAA and CAA-related hemorrhages. Furthermore, the lack of ABCA1 in mice may induce changes in the artery wall similar to the atherosclerotic changes in humans (and morphologically distinct from CAA) that could affect the clearance of Aβ through the blood-brain barrier. In addition, atherosclerotic changes in the artery wall could decrease the supply of nutrients to the brain, thus aggravating AD-related pathology. Recent studies revealed the following: 1) AD patients have more severe atherosclerosis than age-matched controls without AD (74), and 2) there is a positive correlation between the degree of atherosclerotic disease of cerebral arteries in AD patients and the neuropathological features typical for the AD patients (74, 75).

In conclusion, the results from our study show that in APP23 mice, ABCA1 disruption substantially increases amyloid deposition in the brain and vasculature, regardless of the very low apoE protein level and possibly through an impaired Aβ clearance. By understanding the complex regulatory network and the cross-talk between cholesterol transporters, brain lipoproteins, and their receptors in the context of APP processing and Aβ clearance, it may be possible to identify new targets for AD therapies.

Acknowledgments—We thank Dr. P. Land (Department of Neurobiology, University of Pittsburgh) for valuable advice and the opportunity to process brain tissue in his laboratory. We thank L. Shamalla (P. Land laboratory) and K.

[5] M. Walter (University of Munster, Germany), personal communication.

Fertig (Department of Pharmacology) for technical support. We also thank Cheryl Wellington and David Holtzman for sharing their results prior to publication.

REFERENCES

1. Olichney, J. M., Hansen, L. A., Galasko, D., Saitoh, T., Hofstetter, C. R., Katzman, R., and Thal, L. J. (1996) *Neurology* **47,** 190–196
2. Bertram, L., and Tanzi, R. E. (2004) *Pharmacol. Res.* **50,** 385–396
3. Yamada, M. (2004) *J. Neurol. Sci.* **226,** 41–44
4. Bales, K. R., Verina, T., Dodel, R. C., Du, Y., Altstiel, L., Bender, M., Hyslop, P., Johnstone, E. M., Little, S. P., Cummins, D. J., Piccardo, P., Ghetti, B., and Paul, S. M. (1997) *Nat. Genet.* **17,** 263–264
5. Bales, K. R., Verina, T., Cummins, D. J., Du, Y., Dodel, R. C., Saura, J., Fishman, C. E., DeLong, C. A., Piccardo, P., Petegnief, V., Ghetti, B., and Paul, S. M. (1999) *Proc. Natl. Acad. Sci. U. S. A.* **96,** 15233–15238
6. Fryer, J. D., Taylor, J. W., DeMattos, R. B., Bales, K. R., Paul, S. M., Parsadanian, M., and Holtzman, D. M. (2003) *J. Neurosci.* **23,** 7889–7896
7. Hirsch-Reinshagen, V., Zhou, S., Burgess, B. L., Bernier, L., McIsaac, S. A., Chan, J. Y., Tansley, G. H., Cohn, J. S., Hayden, M. R., and Wellington, C. L. (2004) *J. Biol. Chem.* **279,** 41197–41207
8. Wahrle, S. E., Jiang, H., Parsadanian, M., Legleiter, J., Han, X., Fryer, J. D., Kowalewski, T., and Holtzman, D. M. (2004) *J. Biol. Chem.* **279,** 40987–40993
9. Repa, J. J., Turley, S. D., Lobaccaro, J. A., Medina, J., Li, L., Lustig, K., Shan, B., Heyman, R. A., Dietschy, J. M., and Mangelsdorf, D. J. (2000) *Science* **289,** 1524–1529
10. Brewer, H. B., Jr., Remaley, A. T., Neufeld, E. B., Basso, F., and Joyce, C. (2004) *Arterioscler. Thromb. Vasc. Biol.* **24,** 1755–1760
11. Rust, S., Rosier, M., Funke, H., Real, J., Amoura, Z., Piette, J. C., Deleuze, J. F., Brewer, H. B., Duverger, N., Denefle, P., and Assmann, G. (1999) *Nat. Genet.* **22,** 352–355
12. Brooks-Wilson, A., Marcil, M., Clee, S. M., Zhang, L. H., Roomp, K., van Dam, M., Yu, L., Brewer, C., Collins, J. A., Molhuizen, H. O., Loubser, O., Ouelette, B. F., Fichter, K., Ashbourne-Excoffon, K. J., Sensen, C. W., Scherer, S., Mott, S., Denis, M., Martindale, D., Frohlich, J., Morgan, K., Koop, B., Pimstone, S., Kastelein, J. J., and Hayden, M. R. (1999) *Nat. Genet.* **22,** 336–345
13. Bodzioch, M., Orso, E., Klucken, J., Langmann, T., Bottcher, A., Diederich, W., Drobnik, W., Barlage, S., Buchler, C., Porsch-Ozcurumez, M., Kaminski, W. E., Hahmann, H. W., Oette, K., Rothe, G., Aslanidis, C., Lackner, K. J., and Schmitz, G. (1999) *Nat. Genet.* **22,** 347–351
14. Tontonoz, P., and Mangelsdorf, D. J. (2003) *Mol. Endocrinol.* **17,** 985–993
15. Wang, N., and Tall, A. R. (2003) *Arterioscler. Thromb. Vasc. Biol.* **23,** 1178–1184
16. Koldamova, R. P., Lefterov, I. M., Ikonomovic, M. D., Skoko, J., Lefterov, P. I., Isanski, B. A., DeKosky, S. T., and Lazo, J. S. (2003) *J. Biol. Chem.* **278,** 13244–13256
17. Sun, Y., Yao, J., Kim, T. W., and Tall, A. R. (2003) *J. Biol. Chem.* **278,** 27688–27694
18. Brown, J., III, Theisler, C., Silberman, S., Magnuson, D., Gottardi-Littell, N., Lee, J. M., Yager, D., Crowley, J., Sambamurti, K., Rahman, M. M., Reiss, A. B., Eckman, C. B., and Wolozin, B. (2004) *J. Biol. Chem.* **279,** 34674–34681
19. Katzov, H., Chalmers, K., Palmgren, J., Andreasen, N., Johansson, B., Cairns, N. J., Gatz, M., Wilcock, G. K., Love, S., Pedersen, N. L., Brookes, A. J., Blennow, K., Kehoe, P. G., and Prince, J. A. (2004) *Hum. Mutat.* **23,** 358–367
20. Wollmer, M. A., Streffer, J. R., Lutjohann, D., Tsolaki, M., Iakovidou, V., Hegi, T., Pasch, T., Jung, H. H., Bergmann, K., Nitsch, R. M., Hock, C., and Papassotiropoulos, A. (2003) *Neurobiol. Aging* **24,** 421–426
21. Li, Y., Tacey, K., Doil, L., Luchene, R. V., Garcia, V., Rowland, C., Schrodi, S., Leong, D., Lau, K., and Catanese, J. (2004) *Neurosci. Lett.* **366,** 268–271
22. Van Dam, D., Vloeberghs, E., Abramowski, D., Staufenbiel, M., and De Deyn, P. P. (2005) *CNS. Spectr.* **10,** 207–222
23. Sturchler-Pierrat, C., Abramowski, D., Duke, M., Wiederhold, K. H., Mistl, C., Rothacher, S., Ledermann, B., Burki, K., Frey, P., Paganetti, P. A., Waridel, C., Calhoun, M. E., Jucker, M., Probst, A., Staufenbiel, M., and Sommer, B. (1997) *Proc. Natl. Acad. Sci. U. S. A.* **94,** 13287–13292
24. Sturchler-Pierrat, C., and Staufenbiel, M. (2000) *Ann. N. Y. Acad. Sci.* **920,** 134–139
25. Koldamova, R. P., Lefterov, I. M., Staufenbiel, M., Wolfe, D., Huang, S., Glorioso, J. C., Walter, M., Roth, M. G., and Lazo, J. S. (2005) *J. Biol. Chem.* **280,** 4079–4088
26. Matsuoka, Y., Picciano, M., Malester, B., LaFrancois, J., Zehr, C., Daeschner, J. M., Olschowka, J. A., Fonseca, M. I., O'Banion, M. K., Tenner, A. J., Lemere, C. A., and Duff, K. (2001) *Am. J. Pathol.* **158,** 1345–1354
27. Bussiere, T., Bard, F., Barbour, R., Grajeda, H., Guido, T., Khan, K., Schenk, D., Games, D., Seubert, P., and Buttini, M. (2004) *Am. J. Pathol.* **165,** 987–995
28. Calhoun, M. E., Burgermeister, P., Phinney, A. L., Stalder, M., Tolnay, M., Wiederhold, K. H., Abramowski, D., Sturchler-Pierrat, C., Sommer, B., Staufenbiel, M., and Jucker, M. (1999) *Proc. Natl. Acad. Sci. U. S. A.* **96,** 14088–14093
29. Carson, F. L. (1996) *Histotechnology: A Self-Instructional Text*, 2nd Ed., ASCP, Chicago
30. Burns, M. P., Noble, W. J., Olm, V., Gaynor, K., Casey, E., LaFrancois, J., Wang, L., and Duff, K. (2003) *Mol. Brain Res.* **110,** 119–125
31. Kuo, Y. M., Beach, T. G., Sue, L. I., Scott, S., Layne, K. J., Kokjohn, T. A., Kalback, W. M., Luehrs, D. C., Vishnivetskaya, T. A., Abramowski, D., Sturchler-Pierrat, C., Staufenbiel, M., Weller, R. O., and Roher, A. E. (2001) *Mol. Med.* **7,** 609–618
32. Calhoun, M. E., Wiederhold, K. H., Abramowski, D., Phinney, A. L., Probst, A., Sturchler-Pierrat, C., Staufenbiel, M., Sommer, B., and Jucker, M. (1998) *Nature* **395,** 755–756
33. Holtzman, D. M., Fagan, A. M., Mackey, B., Tenkova, T., Sartorius, L., Paul, S. M., Bales, K., Ashe, K. H., Irizarry, M. C., and Hyman, B. T. (2000) *Ann. Neurol.* **47,** 739–747
34. Holtzman, D. M., Bales, K. R., Tenkova, T., Fagan, A. M., Parsadanian, M., Sartorius, L. J., Mackey, B., Olney, J., McKeel, D., Wozniak, D., and Paul, S. M. (2000) *Proc. Natl. Acad. Sci. U. S. A.* **97,** 2892–2897
35. Winkler, D. T., Bondolfi, L., Herzig, M. C., Jann, L., Calhoun, M. E., Wiederhold, K. H., Tolnay, M., Staufenbiel, M., and Jucker, M. (2001) *J. Neurosci.* **21,** 1619–1627
36. Koeppen, A. H. (1995) *J. Neurol. Sci.* **134,** 1–9
37. Kivipelto, M., Helkala, E. L., Laakso, M. P., Hanninen, T., Hallikainen, M., Alhainen, K., Soininen, H., Tuomilehto, J., and Nissinen, A. (2001) *BMJ* **322,** 1447–1451
38. Pappolla, M. A., Bryant-Thomas, T. K., Herbert, D., Pacheco, J., Fabra, G. M., Manjon, M., Girones, X., Henry, T. L., Matsubara, E., Zambon, D., Wolozin, B., Sano, M., Cruz-Sanchez, F. F., Thal, L. J., Petanceska, S. S., and Refolo, L. M. (2003) *Neurology* **61,** 199–205
39. Gorelick, P. B. (2004) *Stroke* **35,** 2620–2622
40. Emery, V. O., Gillie, E. X., and Smith, J. A. (2005) *J. Neurol. Sci.* **229,** 27–36
41. Humphries, S. E., and Morgan, L. (2004) *Lancet Neurol.* **3,** 227–235
42. Singaraja, R. R., Brunham, L. R., Visscher, H., Kastelein, J. J., and Hayden, M. R. (2003) *Arterioscler. Thromb. Vasc. Biol.* **23,** 1322–1332
43. Clee, S. M., Zwinderman, A. H., Engert, J. C., Zwarts, K. Y., Molhuizen, H. O., Roomp, K., Jukema, J. W., van Wijland, M., van Dam, M., Hudson, T. J., Brooks-Wilson, A., Genest, J., Jr., Kastelein, J. J., and Hayden, M. R. (2001) *Circulation* **103,** 1198–1205
44. Zlokovic, B. V. (2005) *Trends Neurosci.* **28,** 202–208
45. Games, D., Adams, D., Alessandrini, R., Barbour, R., Borthelette, P., Blackwell, C., Carr, T., Clemens, J., Donaldson, T., Gillespie, F., Guido, T., Hagopian, S., Johnson-Wood, K., Khan, K., Lee, M., Leibowitz, P., Lieberburg, I., Little, S., Masliah, E., McConlogue, L., Montoya-Zavala, M., Mucke, L., Paganini, L., Penniman, E., Power, M., Schenk, D., Seubert, P., Snyder, B., Soriano, F., Tan, H., Vitale, J., Wadsworth, S., Wolozin, B., and Zhao, J. (1995) *Nature* **373,** 523–527
46. Davis, J., Xu, F., Deane, R., Romanov, G., Previti, M. L., Zeigler, K., Zlokovic, B. V., and Van Nostrand, W. E. (2004) *J. Biol. Chem.* **279,** 20296–20306
47. Jankowsky, J. L., Fadale, D. J., Anderson, J., Xu, G. M., Gonzales, V., Jenkins, N. A., Copeland, N. G., Lee, M. K., Younkin, L. H., Wagner, S. L., Younkin, S. G., and Borchelt, D. R. (2004) *Hum. Mol. Genet.* **13,** 159–170
48. Shibata, M., Yamada, S., Kumar, S. R., Calero, M., Bading, J., Frangione, B., Holtzman, D. M., Miller, C. A., Strickland, D. K., Ghiso, J., and Zlokovic, B. V. (2000) *J. Clin. Investig.* **106,** 1489–1499
49. Dietschy, J. M., and Turley, S. D. (2004) *J. Lipid Res.* **45,** 1375–1397
50. Rye, K. A., and Barter, P. J. (2004) *Arterioscler. Thromb. Vasc. Biol.* **24,** 421–428
51. DeMattos, R. B., Cirrito, J. R., Parsadanian, M., May, P. C., O'Dell, M. A., Taylor, J. W., Harmony, J. A., Aronow, B. J., Bales, K. R., Paul, S. M., and Holtzman, D. M. (2004) *Neuron* **41,** 193–202
52. Deane, R., Wu, Z., Sagare, A., Davis, J., Du, Y. S., Hamm, K., Xu, F., Parisi, M., LaRue, B., Hu, H. W., Spijkers, P., Guo, H., Song, X., Lenting, P. J., Van Nostrand, W. E., and Zlokovic, B. V. (2004) *Neuron* **43,** 333–344
53. Koistinaho, M., Lin, S., Wu, X., Esterman, M., Koger, D., Hanson, J., Higgs, R., Liu, F., Malkani, S., Bales, K. R., and Paul, S. M. (2004) *Nat. Med.* **10,** 719–726
54. Ruiz, J., Kouiavskaia, D., Migliorini, M., Robinson, S., Saenko, E. L., Gorlatova, N., Li, D., Lawrence, D., Hyman, B. T., Weisgraber, K. H., and Strickland, D. K. (2005) *J. Lipid Res.* **46,** 1721–1731
55. LaDu, M. J., Falduto, M. T., Manelli, A. M., Reardon, C. A., Getz, G. S., and Frail, D. E. (1994) *J. Biol. Chem.* **269,** 23403–23406
56. LaDu, M. J., Pederson, T. M., Frail, D. E., Reardon, C. A., Getz, G. S., and Falduto, M. T. (1995) *J. Biol. Chem.* **270,** 9039–9042
57. Koudinov, A. R., Berezov, T. T., Kumar, A., and Koudinova, N. V. (1998) *Clin. Chim. Acta* **270,** 75–84
58. Koudinov, A. R., Berezov, T. T., and Koudinova, N. V. (2001) *Neurosci. Lett.* **314,** 115–118
59. Koldamova, R. P., Lefterov, I. M., Lefterova, M. I., and Lazo, J. S. (2001) *Biochemistry* **40,** 3553–3560
60. Maezawa, I., Jin, L. W., Woltjer, R. L., Maeda, N., Martin, G. M., Montine, T. J., and Montine, K. S. (2004) *J. Neurochem.* **91,** 1312–1321
61. McNeish, J., Aiello, R. J., Guyot, D., Turi, T., Gabel, C., Aldinger, C., Hoppe, K. L., Roach, M. L., Royer, L. J., de Wet, J., Broccardo, C., Chimini, G., and Francone, O. L. (2000) *Proc. Natl. Acad. Sci. U. S. A.* **97,** 4245–4250
62. Wolf, H., Hensel, A., Arendt, T., Kivipelto, M., Winblad, B., and Gertz, H. J. (2004) *Ann. Neurol.* **56,** 745–748
63. Hasty, A. H., Plummer, M. R., Weisgraber, K. H., Linton, M. F., Fazio, S., and Swift,

L. L. (2005) *J. Lipid Res.* **46,** 1433–1439
64. Fagan, A. M., Christopher, E., Taylor, J. W., Parsadanian, M., Spinner, M., Watson, M., Fryer, J. D., Wahrle, S., Bales, K. R., Paul, S. M., and Holtzman, D. M. (2004) *Am. J. Pathol.* **165,** 1413–1422
65. Koenigsknecht, J., and Landreth, G. (2004) *J. Neurosci.* **24,** 9838–9846
66. Bamberger, M. E., Harris, M. E., McDonald, D. R., Husemann, J., and Landreth, G. E. (2003) *J. Neurosci.* **23,** 2665–2674
67. Bornemann, K. D., Wiederhold, K. H., Pauli, C., Ermini, F., Stalder, M., Schnell, L., Sommer, B., Jucker, M., and Staufenbiel, M. (2001) *Am. J. Pathol.* **158,** 63–73
68. Hamon, Y., Broccardo, C., Chambenoit, O., Luciani, M. F., Toti, F., Chaslin, S., Freyssinet, J. M., Devaux, P. F., McNeish, J., Marguet, D., and Chimini, G. (2000) *Nat. Cell Biol.* **2,** 399–406
69. Kinchen, J. M., Cabello, J., Klingele, D., Wong, K., Feichtinger, R., Schnabel, H., Schnabel, R., and Hengartner, M. O. (2005) *Nature* **434,** 93–99
70. Reddy, S. T., Hama, S., Ng, C., Grijalva, V., Navab, M., and Fogelman, A. M. (2002) *Arterioscler. Thromb. Vasc. Biol.* **22,** 1877–1883
71. Wisniewski, H., Wegiel, J., Vorbrodt, A. W., and Frackowiak, J. (2000) *Ann. N. Y. Acad. Sci.* **903,** 6–18
72. Miao, J., Vitek, M. P., Xu, F., Previti, M. L., Davis, J., and Van Nostrand, W. E. (2005) *J. Neurosci.* **25,** 6271–6277
73. Van Nostrand, W. E., Melchor, J. P., and Ruffini, L. (1998) *J. Neurochem.* **70,** 216–223
74. Roher, A. E., Esh, C., Rahman, A., Kokjohn, T. A., and Beach, T. G. (2004) *Stroke* **35,** 2623–2627
75. Honig, L. S., Kukull, W., and Mayeux, R. (2005) *Neurology* **64,** 494–500
76. Wahrle, S. E., Jiang, H., Parsadanian, M., Hartman, R. E., Bales, K. R., Paul, S. M., and Holtzman, D. M. (2005) *J. Biol. Chem.* **280,** 43236–43242
77. Hirsch-Reinshagen, V., Maia, L. F., Burgess, B. L., Blain, J.-F., Naus, K. E., McIsaac, S. A., Parkinson, P. F., Chan, J. Y., Tansley, G. H., Hayden, M. R., Poirier, J., Van Nostrand, W., and Wellington, C. L. (2005) *J. Biol. Chem.* **280,** 43243–43256